Quantitative Theory for Linear Dynamics of Linear Entangled Polymers

Alexei E. Likhtman* and Tom C. B. McLeish

Physics Department, University of Leeds, Leeds LS2 9JT, UK

Received January 7, 2002; Revised Manuscript Received May 13, 2002

ABSTRACT: We present a new quantitative development of the reptation picture of de Gennes−Doi−Edwards. It is well-known that the original reptation theory is unable to fit linear relaxation spectra (G' and G'') as it misses several important physical processes: (1) contour length fluctuations, (2) constraint release, and (3) longitudinal stress relaxation along the tube. All of these processes were treated theoretically before; however, the treatment used either uncontrolled approximations or failed to include all of them at the same time. The aim of this work is to combine self-consistent theories for contour length fluctuations and constraint release with reptation theory. First, we improve the treatment of contour length fluctuations using a combined theoretical and stochastic simulation approach. This allows us to obtain an expression for the single chain relaxation function $\mu(t)$ without any adjustable parameters and approximations. To include constraint release, we use the scheme proposed by Rubinstein and Colby, which provides an algorithm for calculating the full relaxation function $G(t)$ from the single chain relaxation $\mu(t)$. Then longitudinal modes are added, and a detailed comparison with different experimental data is given. One of the conclusions is that polystyrene is described by theory very well, but polybutadiene shows problems, which may be a first indication of nonuniversality of polymer dynamics.

1. Introduction

During the past two decades, theoretical efforts in describing dynamics of entangled polymer melts have been dominated by a sequence of improvements of the reptation theory of de Gennes[1] and Doi and Edwards.[2] Reptation theory consists of three main assumptions: first is that all other chains surrounding one particular chain are replaced by an effective field (the mean field approach), which acts as a tube around the particular chain and prohibits its motion in directions perpendicular to the primitive path. The second assumption is that longitudinal motion along the tube is reptation, which is simultaneous motion of all monomers; i.e., the polymer chain is replaced by the flexible rod with fixed length and only one degree of freedom (Figure 1a). The third is that chain ends are not affected by topological constraints from other chains and, via reptation, occupy new tube segments selected from an isotropic distribution.

The two main improvements to the reptation theory are well-known and were proposed at the same time as reptation theory was published. First is "constraint release" (CR), which is the self-consistent closure of the mean-field picture: because the tube is made from other chains which are moving around, the tube must also move. In particular, it was proposed by de Gennes[3] that the tube motion should be similar to Rouse-like motion with the temperature replaced by the frequency of constraint release. The most detailed self-consistent theory for constraint release was developed by Rubinstein and Colby,[7] where they model the tube motion as a motion of Rouse chain with mobilities distributed according to the solution of the single chain problem. We will revisit this approach in section 4.

The second improvement is the inclusion of contour-length fluctuations (CLF), which corresponds to a more detailed description of the single chain motion inside the tube. If the chain is flexible enough to be considered as Gaussian, then it can be modeled as one-dimensional Rouse chain consisting from beads and springs (Figure 1b). Reptation motion is a motion of the center of mass, i.e., of the *zeroth* Rouse mode. The inclusion of all other Rouse modes leads to fluctuations of the path length of occupied tube segments and to the more complicated dynamics of the chain escape from the tube. Despite the fact that the object of the problem seems to be very simple (1-d Rouse chain), the exact solution is still not known. The first theoretical attempt to calculate the effect of CLF was made by Doi,[4,5] where he estimated the effect of CLF on reptation behavior and proposed an approximation for the early time behavior. Since Doi, most treatments of CLF[6,7] were based on his assumptions; in particular, the expression in ref 6 for the typical relaxation time of a segment near a chain end by CLF is different from Doi's only because of the different definition of number of entanglements N_e. An alternative theory was proposed by des Cloizeaux[13] where he replaced many mode problem by one mode but with a time-dependent diffusion coefficient. We shall compare our theory with these two approaches and show that

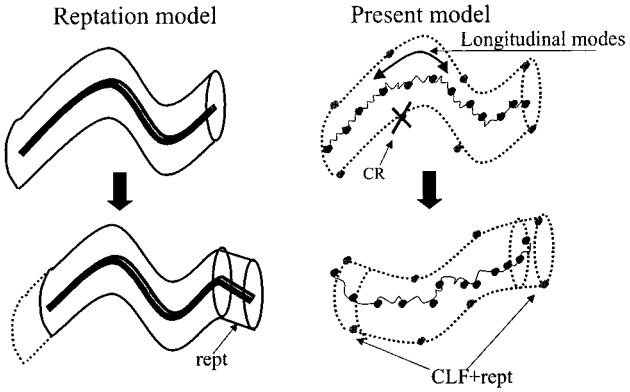

Figure 1. Schematic illustration of reptation (a) and current model which combines reptation, contour length fluctuations, constraint release, and longitudinal modes (b).

* Corresponding author: e-mail A.Likhtman@leeds.ac.uk.

10.1021/ma0200219 CCC: $22.00
Published on Web 06/28/2002

neither of them solves the one-chain problem with the accuracy now required to make comparison to experiment. Rubinstein and Colby, in their sophisticated treatment of CR,[7] also addressed CLF, but using approximations poorer than that of ref 6.

Another addition to the reptation theory is a longitudinal stress relaxation, which was addressed in ref 6, but via postulate rather than calculation. This stress relaxation originates from the fact that because different tube segments before deformation are oriented differently, they also stretch differently, and therefore after the deformation a process of redistribution of monomers along the tube takes place. This process is active for times up to the Rouse time and, as we show in section 5, is responsible for the relaxation of $^1/_5$ of the stress stored in the tubes (in contrast to the assumed value of $^1/_3$ in ref 6).

The mechanisms described above are relatively well established, and there is more or less a consensus in the scientific community about what mathematical model must be solved. Therefore, the aim of this paper is not to introduce any new physical processes but rather to solve the existing mathematical models self-consistently and with the maximal accuracy in each case simultaneously. The special feature of this work is an emphasis on the approximations used and a careful estimation of errors which were therefore originated. As a result, we obtain the expression for relaxation moduli G' and G'', which solves the described mathematical model with precision of about 5% over the entire frequency range from local Rouse motion to the terminal zone. This precision does not mean of course that the mathematical model under consideration describes real polymer melt with this accuracy. We then compare it to several sets of experimental data. We shall draw attention to areas of disagreement with the theory rather than proclaim happy agreement of everything and argue that the remaining disagreement in some cases must be attributed to physical processes not included in the model or to the experimental difficulties, but not to the mathematical approximations used before.

We have another purpose in mind in this work, which concerns the experimental characterization of polymer melts and its relation to theory. In particular, we will show how definitions of the "plateau modulus" $G_N^{(0)}$ need to be made more carefully than has often been the case. We also recommend both notation and definitions that are consistent with the tube theory and simplify theoretical expressions used in the field.

In the next section we describe the mathematical model of the polymer melt and discuss the definitions of the number of entanglements, the tube diameter, and the plateau modulus. In the third section we solve the one-chain problem (reptation + CLF) combining analytical and stochastic approaches. In the fourth section we incorporate constraint release by using the approach of ref 7. In the fifth section we calculate stress relaxation due to longitudinal modes, and in the sixth we discuss the results for G' and G'' and plot different experimental quantities usually extracted from them. Section 7 compares the theoretical predictions with published sets of experimental data, and conclusions are discussed in section 8. Appendix A provides details of calculations used in section 5, and Appendix B discusses possible ways of determining tube persistence length a from simulations and incoherent neutron scattering.

2. The Model, Moduli, and Entanglement Density

The model we are trying to solve is the following. Each chain consists of N beads with friction coefficient ζ, connected by springs with spring constant $3k_BT/b^2$, where b is the Kuhn segment and T is the temperature. Each chain is confined to the tube, which is a random Gaussian walk with effective persistence length a, assumed to be equal to the tube diameter. This assumption is based on the argument of the isotropy of the entanglement network but depends on the particular picture of the entanglement, therefore we will use it but leave the question about its strict validity open. In Appendix B we show that tube persistence length can be easily defined by measuring mean-squre displacement of a monomer at times smaller and larger than τ_e. There are entropic forces which act on the end monomers of the chain (see for example ref 2), which are equal to $f = 3k_BT/a$ and therefore create nonzero average tube length L_0 for each chain. From these parameters we conclude that each tube segment contains $N_e = a^2/b^2$ monomers, that the number of tube segments is $Z = N/N_e = Nb^2/a^2$, and that the average tube length is $L_0 = Za = Nb^2/a$. Note the absence of any prefactors in these definitions.

If the Z entanglements per chain were cross-links, then rubber elasticity theory, which assumes affine deformation of cross-links, would predict the plateau (shear) modulus to be

$$G_N^{(0)\text{Ferry}} = \frac{\rho RT}{M_e} \tag{1}$$

where $M_e = M/Z$ and M is a molar mass of the chain. This equation was used by Ferry to define number of entanglements. The applicability of the affine network model to the entangled polymers is an approximation which is under discussion at the moment;[8] however, we assume it for this paper following most of the previous work on entangled polymers. Doi−Edwards theory predicts the plateau modulus to be $^4/_5$ of the rubber modulus, eq 1, because entanglements do allow longitudinal motion along the tube and are hence different from cross-links:

$$G_N^{(0)\text{Graessley}} = \frac{4}{5}\frac{\rho RT}{M_e} \tag{2}$$

(Graessley used this equation to define M_e.) We conclude that Doi−Edwards theory predicts that $^1/_5$ of the stress stored in the tubes after deformation is relaxed by longitudinal modes. However, the dynamics of this process were not calculated. Moreover, it was stated in ref 2 that longitudinal modes are relaxed at time scale of $\tau_e = N_e^2\zeta b^2/(3\pi^2 k_BT)$, which is the Rouse time of the chain segment between entanglements. In section 5, we calculate precisely the dynamics of longitudinal modes and show that they relax only after the Rouse time of the whole chain. However, at this time scale all other mechanisms are acting, such as contour length fluctuations and constraint release. We thus conclude that the definition of the plateau modulus $G_N^{(0)}$ as the stress at the moment of time after relaxation of longitudinal modes but before escape from the tube via CLF is inconsistent. A more secure definable experimental quantity is the "entanglement modulus" $G_e = \sigma(\tau_e)/\gamma$, i.e., the stress before relaxation of the longitudinal

modes. G_e is defined considering entanglements as a cross-links and so is expressed in terms of M_e by eq 1. However, thus defined G_e is about 20% higher than a visual plateau in G'. (The exact value will depend on Z, as we shall see.) Therefore, we suggest wider use of the entanglement modulus G_e and leave the notation of plateau modulus $G_N^{(0)}$ for the experimentally observed plateau of G'. We will discuss their relation in section 6, in particular Figure 9b. But we note that it is essential that the entanglement molecular weight M_e is defined via G_e without $^4/_5$ prefactors and not via $G_N^{(0)}$.

Although this definition is different from the "theoretical" definition eq 2, it has an additional advantage that the $^4/_5$ prefactor does not appear in any relation of a, N_e, and G_e. We summarize those once again

$$a^2 = N_e b^2; \quad G_e = \frac{\rho R T}{M_e}; \quad Z = \frac{N}{N_e}; \quad L_0 = Za \qquad (3)$$

Note also that introduction of the factor of $^4/_5$ in the definition of N_e led to an erroneous reptation contribution in ref 6. We should add that the adoption of eq 2 as a definition of M_e has been suggested by Graessley[11] and recently implemented by Fetters[12] in place of the older form of eq 1. Our proposal will be that M_e be better defined via G_e, although this will turn out to be closer to definition eq 2 than eq 1.

The last thing which needs to be added in the model is the tube motion due to constraint release, which we discuss in detail in section 4 and show that we need one more numerical parameter c_ν, which is connected to the number of chains that are needed to create one entanglement.

3. Single Chain Problem

We start our solution of the full problem from calculating the tube-segment occupation function $\mu(t)$ due to escape of the single chain from its original tube, which is proportional to the stress relaxation function if one neglects constraint release. As in all tube theories $\mu(t) = L(t)/L_0$; i.e., it is equal to the fraction of the tube segments that was not visited by a chain end during time t. Reptation alone leads to the well-known result[2]

$$\mu_{rept}(t) = \sum_{p,\text{odd}} \frac{8}{\pi^2 p^2} \exp\left(-\frac{p^2 t}{\tau_d^{(0)}}\right); \qquad \tau_d^{(0)} = Z^3 \frac{N_e^2 \zeta b^2}{\pi^2 k_B T} = 3Z^3 \tau_e \qquad (4)$$

where $\tau_d^{(0)}$ is the reptation or disentanglement time. The question is how to incorporate all Rouse modes of the chain motion rather than only the zeroth one: the problem of contour length fluctuations. The problem is subdivided into two: the early time ($t < \tau_R$) behavior of $\mu(t)$ and the effect of CLF on the late time relaxation. The second issue was addressed by Doi,[5] and he predicted that $\mu(t)$ at times larger that τ_R should look like renormalized reptation

$$\mu(t > \tau_R) = \tilde{G}_f(Z) \sum_{p,\text{odd}} \frac{8}{\pi^2 p^2} \exp\left(-\frac{p^2 t}{\tau_{df}(Z)}\right) \qquad (5)$$

where $\tilde{G}_f(Z)$ and $\tau_{df}(Z)$ are renormalizations of a dimensionless plateau modulus and the reptation time (due to CLF). Doi predicted the following form for these two functions

$$\tau_{df}(Z) = \tau_d^{(0)}\left(1 - \frac{2C_1}{\sqrt{Z}} + \frac{C_2}{Z} + \ldots\right); \qquad \tilde{G}_f(Z) = 1 - \frac{C_3}{\sqrt{Z}} + \ldots \qquad (6)$$

and derived that the coefficient C_1 should be the same as C_3 and must be larger than 1.47. We agree with this conclusion and aim to calculate the numerical prefactors for the whole range of molecular weights $Z = 2 \ldots \infty$.

The early time behavior of the function $\mu(t)$ ($t < \tau_R$) was addressed also by Doi,[4] and all later works[7,6] used his approximations, which we should therefore briefly review. The first key assumption was that the tube segment, which was at the distance x from the end of the tube at the time $t = 0$ has a single-exponential form for its survival probability

$$\mu(x,t) = \exp\left(-\frac{t}{\tau(x)}\right)$$

where $\tau(x)$ is a mean lifetime of the segment x, and the total relaxation function is

$$\mu(t) = \frac{1}{L}\int_0^L \mu(x,t)\, dx$$

The second assumption is that for early time ($t < \tau_R$) $\tau(x)$ can be found by inverting the expression for mean-square displacement $\langle x^2 \rangle = f(t)$. In particular, it is well-known[2] that for $t < \tau_R$

$$\langle x^2 \rangle = \frac{4Nb^2}{3\pi^{3/2}}\sqrt{\frac{t}{\tau_R}} = \frac{4a^2}{3\pi^{3/2}}\sqrt{\frac{t}{\tau_e}}$$

This result emerges from summing over Rouse contributions to the end-monomer displacement. Inverting this relation gives an estimate for the mean lifetime

$$\tau(x) \approx \frac{9\pi^3}{16}\tau_e \frac{x^4}{a^4} \qquad (7)$$

which is the same as τ_{early} in Milner and McLeish,[6] taking into account that a different definition of N_e with $^4/_5$ prefactor was used in ref 6.

However, it is easy to show that for such early times the relaxation process of one particular tube segment is strongly nonexponential, and therefore the mean first-passage time is in fact very different from the time estimated in eq 7. The simplest analytical illustration of the problem would be a one-dimensional Brownian particle with diffusion coefficient D starting at $t = 0$ at the point $x = 0$. Suppose we sought an expression for its mean first passage time at a point $z > 0$. For such a system the naive inversion procedure will give $\tau(z) = z^2/(2D)$, but the correct mean first passage time actually diverges because some particles will go to $x \to -\infty$ and therefore come back after infinitely long time. To prevent the divergence, one could put a rigid wall at $x = -L$ with $L \gg z$. In this case the exact solution is

$$\tau(z) = \frac{1}{D}\left(zL + \frac{z^2}{2}\right)$$

i.e., for the case $L \gg z$ it is $L/z \gg 1$ times larger than predicted by inversion method. It is also possible to solve this problem for the distribution of relaxation times and show that it is very broad (in fact, $P(\tau) \sim 1/\sqrt{\tau}$ for $z^2/D < \tau < zL/D$), and therefore the single relaxation time approximation is not useful. It is much more complicated to extend this example quantitatively to the motion of the end of the polymer chain, but we conclude that Doi's approach can easily led to the wrong quantitative conclusion.

An alternative approach, which was proposed by des Cloizeaux,[13] is to solve a one-dimensional diffusion equation with a time-dependent diffusion coefficient. The result in notations of this paper is

$$\mu_{\mathrm{dCl}}(t) = \frac{8}{\pi^2}\sum_{p,\mathrm{odd}}\frac{1}{p^2}\exp\left(-\frac{p^2}{\tau_{\mathrm{d}}^{(0)}}\left(t + \tau_{\mathrm{R}}\sum_q\left[\frac{1-\exp\{-q^2t/\tau_{\mathrm{R}}\}}{q^2}\right]\right)\right) \quad (8)$$

However, no arguments to support validity of this approximation were produced. In this paper we will compare our results with this equation.

Therefore, we use a different combined approach to calculate relaxation function $\mu(t)$. A simple scaling analysis (we thank Alexander Semenov for this suggestion) of the Langevin equation of motion of the Rouse chain stretched by the ends with the constant force $f = 3k_{\mathrm{B}}T/a$

$$\zeta\frac{\partial R}{\partial t} = \frac{3k_{\mathrm{B}}T}{b^2}\frac{\partial^2 R}{\partial i^2} + f(i,t);$$
$$\langle f(i,t)\, f(\tilde{i},\tilde{t})\rangle = 2k_{\mathrm{B}}T\zeta\delta(i-\tilde{i})\,\delta(t-\tilde{t}); \quad \frac{\partial R}{\partial i} = a \quad (9)$$

shows that it is invariant under the scaling transformation

$$t = \lambda t'; \quad R = \lambda^{1/4}R'; \quad i = \lambda^{1/2}i' \quad (10)$$

where i is a monomer number and R is its coordinate. We also used a formula $\delta(\lambda(i-\tilde{\imath})) = (1/\lambda)\delta(i-\tilde{\imath})$. This transformation is valid for times less than the Rouse time because otherwise the motion of one end will be affected by the other end. From the transformation eq 10 we conclude that $\mu(t)$ for early time should have a simple scaling form

$$\mu(t) = \frac{L(t)}{L_0} = \frac{L_0 - 2\Delta L(t)}{L_0} = 1 - \frac{C_\mu}{Z}\left(\frac{t}{\tau_{\mathrm{e}}}\right)^{1/4} \quad \text{for } t < \tau_{\mathrm{R}} \quad (11)$$

since the length of the tube visited by each end $\Delta L(t)$ should not depend on the tube length and Z; therefore, τ_{e} is the only time scale, Z enters only via $L_0 = Za$, and C_μ is an unknown numerical prefactor. At long times $t > \tau_{\mathrm{R}}$, $\mu(t)$ should behave according to eq 5 with the as-yet unknown prefactors of eq 6.

In this paper we propose and report results from a relatively simple way for obtaining these unknown prefactors using direct stochastic simulation of eq 9. For each value of Z we simulate the motion of N beads. We divide an x-axis into small segments and store the last time each segment was visited by the chain end, i.e., a current "age" of the segment. At each step $\mu^{\mathrm{instant}}(t)$ is equal to the fraction of segments that live (i.e., remain between two chain ends) more than time t. The resulting $\mu(t)$ is the average of $\mu^{\mathrm{instant}}(t)$ for a long time. To obtain quantitatively correct results, we extrapolate from the simulations to take the simultaneous limit $N \to \infty$ and time step $\Delta t \to 0$ by fitting for each time $\mu(t,N)$ as a function of $1/\sqrt{N}$ by second-order polynomial and taking its value for $1/\sqrt{N} = 0$. Alternatively, we fit each $\mu(t,N)$ with eq 13 described below with two parameters $\tau_{\mathrm{d}f}/\tau_{\mathrm{d}}^{(0)}$ and $\tilde{G}_f$ for $N = 10$, 20, 30, 50, and 100 and then extrapolate their values to $N \to \infty$. This procedure reliably reproduces analytically known values, and the results are stable with respect to its changes and number of points used. The accuracy of the presented calculations for $\mu(t)$ is about 2%, but higher precision can be obtained by collecting more statistics and using more points for extrapolation. We also used an alternative technique of simulating Rouse coordinates and taking a limit of number of Rouse modes leading to infinity. This method gives slightly better convergence, and the results are the same within declared accuracy.

The simulation method we used is not new—analogous simulations were done by Ketzmerick and Öttinger[9] and Ball and O'Connor[10] a long time ago. The new aspect is that we showed that it is possible to combine simulations with analytical predictions in order to get accurate analytical expressions.

The results for $\mu(t)$ for $Z = 3$, 5, 10, 20, 50, 100, and 200 (from left to right) are shown in Figure 2a for the number of Rouse modes 10 and 100 and extrapolated results. Lines show extrapolated results which are indistinguishable in both plots from eq 13.

The behavior of $\mu(t)$ is boring monotonic, and it is difficult to draw any conclusions at the first glance. However, its derivative $\partial\mu/\partial t$ has a power law behavior with its power changing in different regimes. Therefore, in Figure 2b we plot a reduced dimensionless time derivative of the relaxation function $\hat{\mu}(t) \equiv -4Z\tau_{\mathrm{e}}^{1/4}t^{3/4}(\partial\mu/\partial t)$ (form suggested by eq 11), which clearly has a plateau at early times $t < \tau_{\mathrm{R}}$ and reptation behavior $\mu \sim 1\text{-}t^{1/2}$ at later times, which corresponds to the uprise on this graph: $\hat{\mu} \sim t^{1/4}$. We also see that in this plot the early time behavior does not depend on the molecular weight. From fitting early time plateau we get

$$C_\mu = 1.5 \pm 0.02$$

By fitting later time ($t > \tau_{\mathrm{R}}$) parts of the curve with expression 5, we extract the two functions $\tilde{G}_f(Z)$ and $\tau_{\mathrm{d}f}(Z)/\tau_{\mathrm{d}}^{(0)}(Z)$ and then fit them with the third-order polynomial in order to get desired accuracy for the whole Z range

$$\tau_{\mathrm{d}f}(Z)/\tau_{\mathrm{d}}^{(0)}(Z) = 1 - \frac{2C_1}{\sqrt{Z}} + \frac{C_2}{Z} + \frac{C_3}{Z^{3/2}};$$
$$\tilde{G}_f(Z) = 1 - \frac{C_1}{\sqrt{Z}} + \frac{C_4}{Z} + \frac{C_5}{Z^{3/2}} \quad (12)$$

Best fitting of simulations data for $Z = 2\text{–}100$ gives

$$C_1 = 1.69; \quad C_2 = 4.17; \quad C_3 = -1.55; \quad C_4 = 2.0; \quad C_5 = -1.24$$

The extracted values for $\tau_{\mathrm{d}f}$ and $\tilde{G}_f$ and fitting by eq 12 are shown in Figure 3. The five coefficients C_1–C_5 are determined with less precision than C_μ since the fitting

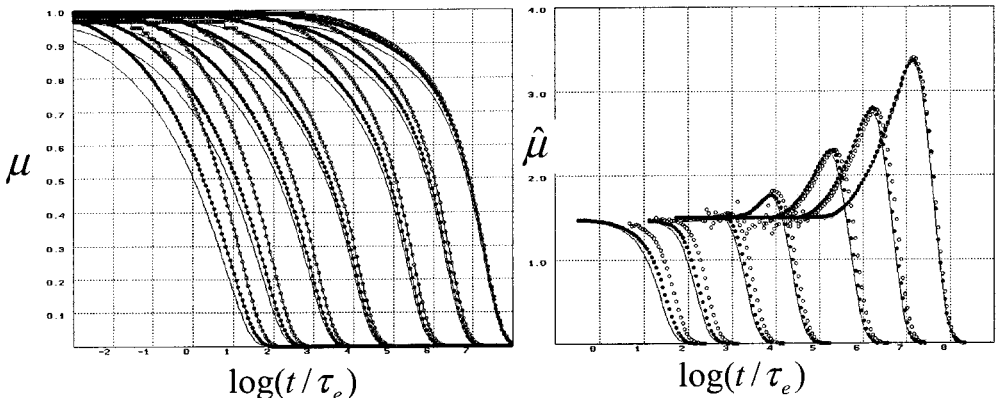

Figure 2. Stochastic results for single chain relaxation function $\mu(t)$ for $Z = 3$, 5, 10, 20, 50, 100, and 200 (from left to right) (a) and its dimensionless derivative $\hat{\mu}(t) \equiv -4Z\tau_e^{1/4}t^{3/4}\,\partial\mu/\partial t$ (b): open symbols, 10 Rouse modes; filled symbols, 100 Rouse modes (30 modes for $Z = 200$); lines, eq 13. The extrapolated results from simulations are indistinguishable from solid lines.

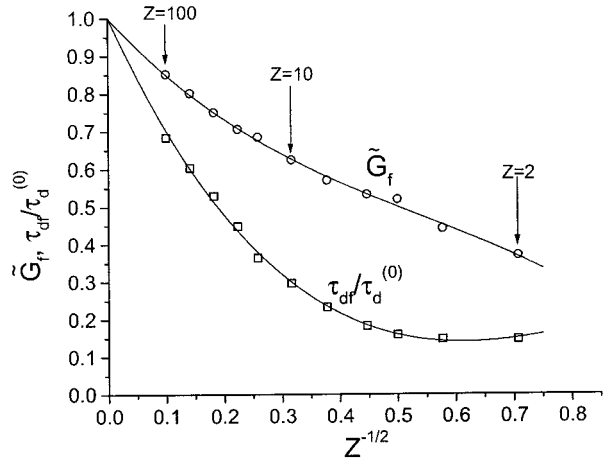

Figure 3. Renormalization of entanglement modulus and reptation time by contour length fluctuation: simulations results (symbols) and fit by eq 12 (lines).

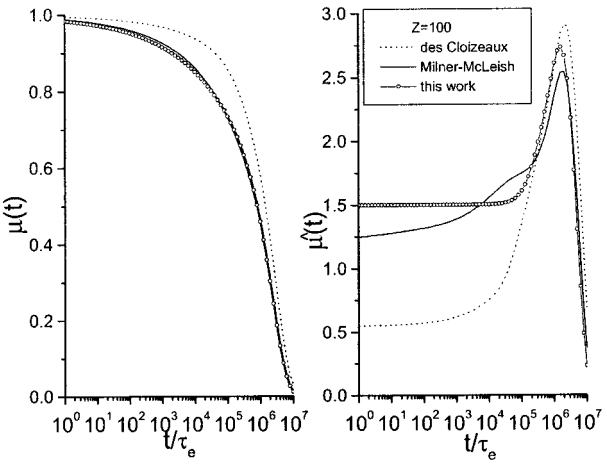

Figure 4. Comparison of results of this paper with results of Doi−Milner−McLeish[6] and des Cloizeaux.[13]

procedure is not unique. However, the proposed combination describes all obtained values with the desired accuracy. The precision of key value C_1 addressed in Doi's work is higher than for other higher-order terms (about 2%). We therefore confirm Doi's result $C_1 > 1.47$.

By fitting $\hat{\mu}(t)$ (which is much more sensitive than $\mu(t)$), we can also propose possible interpolation functions. We note that the transition between the two regimes of CLF and reptation-dominated relaxation within the relaxation spectrum happens exponentially abruptly. Therefore, we propose the simple analytical form which describes $\mu(t)$ at all times

$$\mu(t) = \frac{8\tilde{G}_f}{\pi^2}\sum_{p=1,\mathrm{odd}}^{p^*}\frac{1}{p^2}\exp\left(-\frac{tp^2}{\tau_{df}}\right) + \int_{\epsilon^*}^{\infty}\frac{0.306}{Z\tau_e^{1/4}\epsilon^{5/4}}\exp(-\epsilon t)\,d\epsilon \quad (13)$$

where the prefactor 0.306 is chosen to reproduce the correct early time plateau value of $\hat{\mu}(t)$ and

$$\epsilon^* = \frac{1}{\tau_e Z^4}\left(\frac{4\times 0.306}{1 - 8\tilde{G}_f/\pi^2\sum_{p=1,\mathrm{odd}}^{p^*}\frac{1}{p^2}}\right)^4 \quad (14)$$

is set by the condition $\mu(0) = 1$. We expect that reptation modes are not active at times smaller than Rouse time, so in the reptation component of eq 13 we sum only over modes, such that $\tau_d/p^2 > \tau_R$. This suggests an upper cutoff to the sum $p^* \sim \sqrt{Z}$. The prefactor in p^* is chosen from the fitting to simulations (but we find in practice that results are insensitive to the exact value of this prefactor since inaccurate choice of p^* is compensated for by slight adjustment of ϵ^* according to eq 14). The best fit was given by the specific choice $p^* = \sqrt{Z/10}$. Note that for $Z < 50$ or so only one reptation mode is present. One can see using eq 12 that, in the limit of large Z, $\epsilon^* \approx 1/(3.6\tau_R)$; i.e., contour length fluctuations are not effective after time $3.6\tau_R$.

The results obtained by using eqs 13 and 12 are shown in Figure 2 (lines).

In Figure 4 we compare our results for $\mu(t)$ with predictions of des Cloizeaux (eq 8) and Milner−McLeish[6] (without dynamic dilution) for $Z = 100$. Note that ref 6 contained several misprints and inconsistencies in definitions, which were corrected before comparison.

One can see that the des Cloizeaux relaxation function significantly underestimates the relaxation due to CLF and overestimates τ_{df} and $\tilde{G}_f$ since their renormalization due to CLF was not included. The prediction for $\mu(t)$ by Milner and McLeish[6] is very close to our results for $Z = 100$ but starts to deviate significantly for smaller Z. However, differences can be seen in $\hat{\mu}(t)$. In particular, at early times Milner−McLeish predict $C_\mu = 1.2$ instead of 1.5 obtained in this work. In Figure 5 we compare G' and G'' produced by the single chain relaxation function

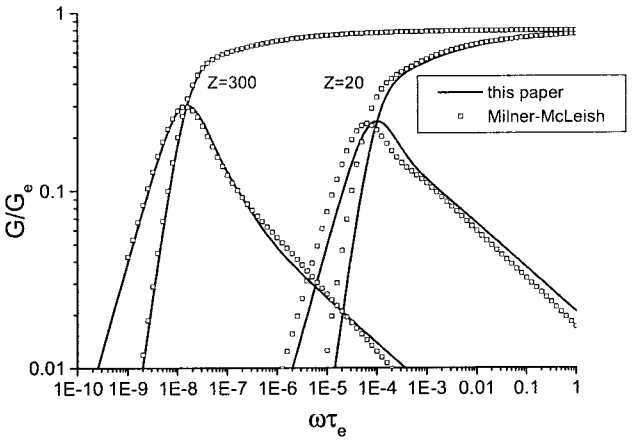

Figure 5. Comparison of results of this paper without CR with results of Milner−McLeish[6] without dynamic dilution.

$\mu(t)$ obtained in this paper with the Milner−McLeish result.[6] One can see that while for long chains the correction is not significant, for shorter chains it is important. For $Z < 20$ both des Cloizeaux and Milner−McLiesh theories give unsatisfactory results. (The agreement for G'' is similar to that of $\hat{\mu}(t)$.)

4. Constraint Release

The escape of one particular chain from its tube affects other chains via the constraint release mechanism. It was proposed a long time ago by de Gennes[3] that constraint release should lead to a Rouse-like motion, but it was also observed[7] that the mobilities of different tube segments are distributed quite widely if one takes into account contour length fluctuations. Therefore, an approximation that all tube segment mobilities are the same $m_i \sim 1/\tau_d$ cannot provide a quantitatively accurate result. The most detailed self-consistent algorithm that obtains the many chain relaxation function $G(t)$ from single chain function $\mu(t)$, and which takes into account the distribution of tube segment mobilities, was developed by Rubinstein and Colby.[7] We review it here briefly and then apply it to our result for $\mu(t)$. In particular, we show that its realization is extremely simple and transparent.

The algorithm of Rubinstein and Colby consists of the following steps. First, one should calculate an inverse Laplace transform for $\mu(t)$, $P(\epsilon)$, so that

$$\mu(t) = \int_0^\infty P(\epsilon) \exp(-\epsilon t)\, d\epsilon$$

and postulate that mobilities of the tube segments m_i are distributed randomly according to $P(\epsilon)$; i.e., $P(\epsilon)\, d\epsilon$ is a fraction of segments with mobility $\epsilon < m < \epsilon + d\epsilon$. $P(\epsilon)$ automatically satisfies the normalization condition $\int P(\epsilon)\, d\epsilon = \mu(0) = 1$.

The second step is to find the spectrum of relaxation rates $M(\epsilon)$ for such a Rouse chain with a set of random mobilities m_i, which was done by using the approach of Dean[15] using Sturm's theorem. ($M(\epsilon)$ is defined as a number of relaxation modes slower than ϵ.) The resulting numerical algorithm is very simple: $M(\epsilon)$ is equal to the number of negative values s_i of the recurrent sequence

$$s_1 = \gamma_1 + \gamma_2 - \epsilon; \quad s_i = \gamma_i + \gamma_{i+1} - \epsilon - \gamma_i^2/s_{i-1} \quad (2 \le i \le Z)$$

where $\gamma_i = (3k_BT/a^2)m_i$.

The third step is to get the relaxation function of the Rouse tube

$$R(t,c_\nu) = \left\langle \int_0^\infty d\epsilon \frac{dM}{d\epsilon} \exp(-\epsilon c_\nu t) \right\rangle \tag{15}$$

where brackets $\langle\,\rangle$ denote averaging over a different realization of mobilities m_i distributed according to $P(\epsilon)$. Here we reintroduce the new dimensionless parameter c_ν analogous to the one used in our nonlinear CCR theory.[14] It reflects the "strength" of the constraint release mechanism, i.e., $c_\nu = 0$, means no constraint release at all; $c_\nu = 1$ corresponds to Rubinstein−Colby theory which assumes that one constraint release event leads to an effective jump of another chain's tube by a distance of the entire tube diameter a. We leave it to be a free parameter since there is no reason to believe that this jump distance is exactly a. In particular, if one entanglement is created by many chains, than escape of one chain will not lead to completely free tube segment, meaning $c_\nu < 1$.

Finally, the resulting many chain relaxation function of the stress accumulated in the tubes is

$$G(t) = \frac{4}{5} G_e R(t,c_\nu)\, \mu(t) \tag{16}$$

(We will discuss the source of $^4/_5$ prefactors in the next section.) This factorized form for the stress relaxation of Rouse dynamics of the tube and entangled dynamics of the chain follows if the two are uncorrelated.[7] One can consider how CR may affect contour length fluctuations and how fluctuations in tension may affect the constraint release. To estimate the importance of the first mechanism, we compare the typical distance which one entanglement segment travels during one reptation time due to reptation $d \sim L = Za$ and due to CR $d \sim a$. Clearly, the CR mechanism is Z times less effective for the motion along the tube. To estimate the influence of tension fluctuations on CR is more problematic. We note that typical fluctuation of tension in one segment is of order of the tension itself. Therefore, fluctuations can moderate CR; however, we expect this fluctuation correction to act as renormalization of the constant c_ν.

The application of a described procedure is straightforward. (We made a choice of $\mu(t)$ judiciously so that it provides a simple inverse Laplace transform.) We simulate a sufficient number of mobility sets for the average in eq 15 for each Z and then calculate $R(t,c_\nu)$ and its contribution to the final $G(t)$. The number of chains simulated in order to get an accurate average in eq 15 was from 300 for short chains to 20 for long ones.

In Figure 6 we plot $R(t)$ together with $\mu(t)$ for $Z = 300$ for $c_\nu = 1$, presented on double-logarithmical axis in a normalized way as $\hat{R}(t) = -4Z\tau_e^{1/4}t^{3/4}\, \partial R/\partial t$ and $\hat{\mu}(t)$. From the second plot we conclude that for early time $t < \tau_R$, $R(t)$ behaves similarly to $\mu(t)$ but with the different prefactor:

$$R(t,c_\nu) = 1 - \frac{C_R}{Z}\left(\frac{c_\nu t}{\tau_e}\right)^{1/4}; \quad C_R \approx 1.8$$

It can also be rewritten as $R(t) \approx \mu(t)^\alpha$ where $\alpha \approx 1.2c_\nu^{1/4}$ and therefore

$$G(t) \approx \mu(t)^{1+\alpha} \quad \text{for } t < \tau_R$$

This equation is very similar to a dynamic dilution or

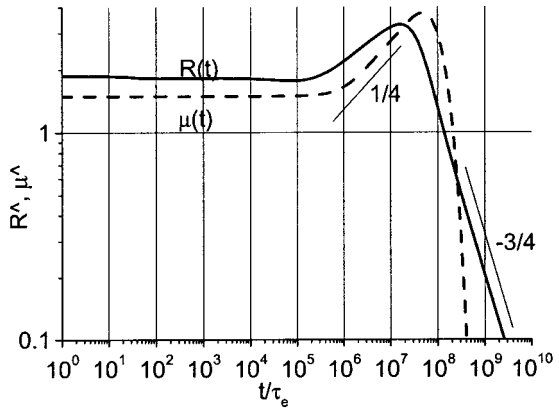

Figure 6. Calculated constraint release relaxation function $R(t)$ (solid line) compared to the single chain relaxation function $\mu(t)$ for $Z = 300$.

double-reptation prediction with an empirical exponent for a dilution power law $G^{(0)} \sim \phi^{1+\alpha}$ with $1 \le \alpha \le {}^4/_3$. Therefore, this result gives a hint that the exponent of $\alpha = {}^4/_3$ may be the result of Rouse-like motion of the tubes rather than due to a nontrivial exponent for dilution. We emphasize however that this approximation is not valid for $t > \tau_R$ and therefore cannot describe the peak shape and terminal time correctly. At large times $R(t)$ behaves like a relaxation function of a normal Rouse chain with $\tau_R^{eff} = \beta\tau_d Z^2$ where $\beta \le 1$ is another prefactor. This means that $R(t)$ has a very long tail with the maximum time $\sim\tau_d Z^2$, at which $\mu(t)$ is exponentially small.

5. Longitudinal Modes of the Stress Relaxation

During small deformation different tube segments are deformed by different amounts because of different initial orientation. This causes redistribution of monomers along the tube after a deformation which relaxes some of the accumulated stress. In this section we calculate the dynamics of this relaxation.

Let us consider a small shear deformation $\mathbf{E}_{\alpha\beta} = \delta_{\alpha\beta} + \gamma\delta_{\alpha 1}\delta_{\beta 2}$ of the tube consisting of Z segments described by unit vectors $\mathbf{u}(s)$, where s is the tube segment number $s = 0...Z$ and $\delta_{\alpha\beta} = 1$ if $\alpha = \beta$, $\delta_{\alpha\beta} = 0$ otherwise. A simple geometrical consideration leads to the stress tensor

$$\sigma_{xy} = \frac{3k_B Tca^2}{Nb^2}\int ds \left\langle \frac{(\mathbf{E}\cdot\mathbf{u})_x(\mathbf{E}\cdot\mathbf{u})_y}{\nu(s,t)} \right\rangle \qquad (17)$$

where $\nu(s,t)$ is the number of monomers in the segment s and c is a number of monomers per unit volume. This is a generalization of the stress expression derived in the Doi−Edwards book[2] (section 7.5.3), where it was erroneously stated that $\nu(s,t)$ becomes constant after Rouse time of one tube segment τ_e. In equilibrium and immediately after the deformation each segment contains $\nu(s, t = +0) = N_e$ monomers. (Any fluctuation correction of this number should be considered separately.) However, after the Rouse time τ_R monomers are redistributed according to segments length to achieve constant chain tension: $\nu(s, t \to \infty) = N_e|\mathbf{Eu}(s)|$. This process of redistribution of monomers along the tube we will call longitudinal stress relaxation. One can calculate the stress tensor immediately after deformation and after longitudinal modes are relaxed:

$$\sigma_{xy} = \frac{3k_B Tc}{N_e}\begin{cases} \langle(\mathbf{E}\cdot\mathbf{u})(\mathbf{E}\cdot\mathbf{u})_y\rangle, & t = +0 \\ \langle(\mathbf{E}\cdot\mathbf{u})_x(\mathbf{E}\cdot\mathbf{u})_y/|\mathbf{E}\cdot\mathbf{u}|\rangle & t \to \infty \end{cases}$$

or taking into account that $\mathbf{Eu} = (u_x + \gamma u_y, u_y, u_z)$ and evaluating integrals over different orientation of u

$$\sigma_{xy} = \frac{Tc}{N_e}\begin{cases} \gamma, & t = +0 \\ {}^4/_5\gamma, & t \to \infty \end{cases}$$

Therefore, ${}^1/_5$ of the stress stored in the tube is relaxed after time τ_R by longitudinal modes. To derive the time dependence of this relaxation, one needs to calculate $\nu(s,t)$. This is done in full in Appendix A. The final result after substitution of $\nu(s,t)$ into eq 17 is that the contribution to the relaxation modulus due to longitudinal modes has a simple "Rouse" form.

$$G^{long}(t) = G_e\left(\frac{4}{5} + \frac{1}{5Z}\sum_{p=1}^{Z}\exp\left(-\frac{p^2 t}{\tau_R}\right)\right) \qquad (18)$$

Although this equation looks rather simple, the main result is that during relaxation of ${}^1/_5$ of the stress each Rouse mode carries the same amount of stress; however, the reason for this is quite different from standard Rouse dynamics. Note that the obtained result is different from the result of ref 6 in the size of the prefactor (${}^1/_5$ here instead of ${}^1/_3$ in ref 6).

6. Results and Discussion

We now combine all processes in the resulting expression for the relaxation modulus

$$G(t) = G_e\left(\frac{4}{5}\mu(t)\,R(t) + \frac{1}{5Z}\sum_{p=1}^{Z-1}\exp\left(-\frac{p^2 t}{\tau_R}\right) + \frac{1}{Z}\sum_{p=Z}^{N}\exp\left(-\frac{2p^2 t}{\tau_R}\right)\right) \qquad (19)$$

where the first term is the contributions due to escape from the tube described by $\mu(t)$ and constraint release described by $R(t)$, the second is longitudinal modes relaxation, and the third is fast Rouse motion inside the tube. Note that in refs 6 and 16 an erroneous expression without the factor of 2 in the exponent was used for the Rouse spectrum. This is of course not insignificant in comparison to data. Storage and loss moduli $G'(\omega)$ and $G''(\omega)$ are found by appropriate Fourier transformation of $G(t)$. Our assumption of pure Rouse motion at high frequency $\omega > \tau_e^{-1}$ is a crude one—experimentally parallel G' and G'' with a slope ${}^1/_2$ are not observed. This is due to glassy dynamics at high frequencies which leads to a wide distribution of Kuhn segment mobilities. Therefore, in comparison with experiment, we only use data at frequencies lower than the high-frequency intersection of G' and G'' and assume that the effect of high-frequency motion on low-frequency region of interest ($\omega < \tau_e^{-1}$) is approximately described by the Rouse model.

In Figure 7, we illustrate the effect of each process on the loss modulus G'' for different numbers of en-

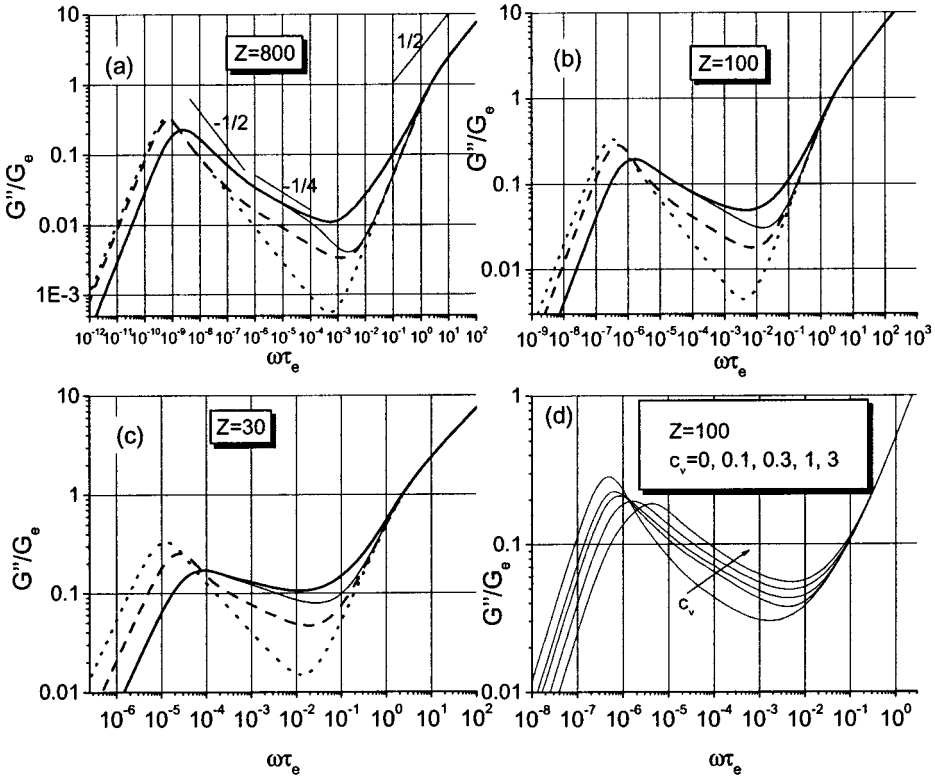

Figure 7. Theoretical prediction for G'' and the influence of different mechanisms for $Z = 800$ (a), $Z = 100$ (b), and $Z = 30$ (c): dotted lines, pure reptation + high-frequency Rouse modes; dashed lines, reptation, CLF, and Rouse; thin solid lines, reptation, CLF, CR, and Rouse; thick solid lines, full model (with longitudinal modes). (d) shows the influence of c_ν parameter on G'' for $Z = 100$.

tanglements $Z = 800$ (a), $Z = 100$ (b), and $Z = 30$ (c), adding the effects one by one according to their significance. The pure reptation + Rouse theory predicts $G'' \sim \omega^{-1/2}$ behavior in the wide region of frequencies. Addition of contour length fluctuations preserves this slope for $\tau_d^{-1} < \omega < \tau_R^{-1}$ but changes it to $-1/4$ for $\omega > \tau_R^{-1}$. Constraint release does not destroy the $-1/4$ dependence (since $R(t) \approx \mu(t)^\alpha$ for $t < \tau_R$) and just shifts G'' up in this region. But it does destroy the $-1/2$ behavior for all realistic Z except of $Z = 800$ by smoothing the peak of G''. Therefore, the behavior $G'' \sim \omega^{-1/2}$ predicted by Doi and Edwards can be observed only for a very high number of entanglements. Finally, addition of longitudinal modes lifts the minimum of G'' up and destroys the $-1/4$ behavior since longitudinal relaxation acts in the same frequency region ($\tau_R^{-1} < \omega < \tau_e^{-1}$) as contour length fluctuations and constraint release; therefore, strictly speaking we do not predict $-1/4$ behavior to be observed anywhere. However, for long enough chains in the vicinity of τ_R the slope of G'' is close to $-1/4$. Figure 7d illustrates the effect of amount of CR in the system described by parameter c_ν. One can see that going from $c_\nu = 0$ to $c_\nu = 0.3$ the peak of G'' becomes smother and lower; in a range $0.3 < c_\nu < 1$ changing c_ν is almost equivalent to changing number of entanglements Z, and for $c_\nu > 2$ the peak shape becomes distorted and asymmetric in contradiction with experiment.

In Figure 8 we plot predicted viscosity $\eta \equiv \int G(t)\,dt$ normalized by the Doi–Edwards prediction $\eta_{DE} = (\pi^2/15)\tau_d^{(0)}G_e$ (a) and steady-state compliance $J_e \equiv (1/\eta^2)\int G(t)t\,dt$. Pure reptation theory predicts $J_eG_e = 3/2$. For

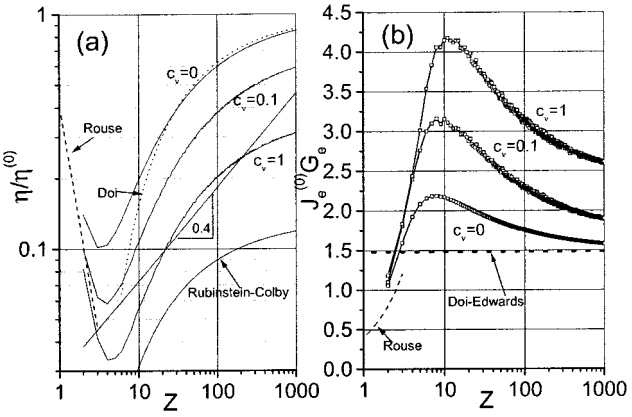

Figure 8. (a) Predictions for viscosity as a function of number of entanglements Z for $c_\nu = 0$, 0.1, and 1. (b) The same for steady-state compliance J_e. Dashed lines show predictions of Rouse theory.

$Z = 1-3$ we also plot the prediction of Rouse theory extracted from

$$G_{Rouse}(t) = \frac{\rho RT}{M}\sum_{p=1}^{N}\exp\left(-\frac{2p^2t}{\tau_R}\right) \rightarrow$$

$$\eta_{Rouse}/\eta_{DE} = \frac{5}{12Z^2}; \quad J^e_{Rouse}G_e = \frac{2}{5}Z$$

For viscosity we note that the shape of the curve is almost independent of the amount of constraint release in the system (c_ν), but CR only shifts the whole curve down. In particular, for $c_\nu = 1$ $\eta(Z \rightarrow \infty) \approx 0.3\eta_{DE}$. The experimental slope of 3.4 (0.4 in this coordinates) is predicted in some range of molecular weights. However,

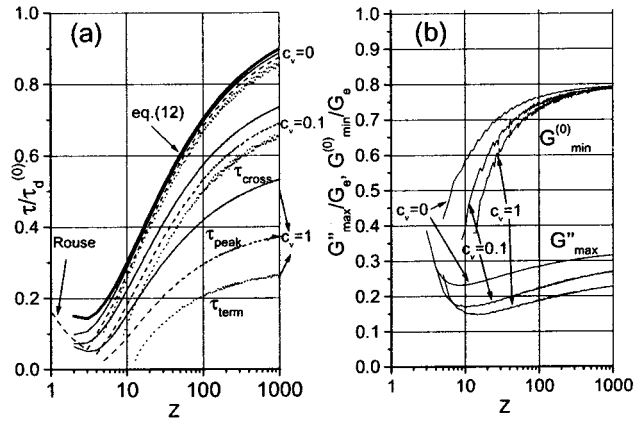

Figure 9. (a) Three different experimental definitions of the terminal time (normalized by pure reptation time) as a function of Z for $c_v = 0$, 0.1, and 1. (b) Experimental definition of the plateau modulus $G^{(0)}_{min}$ and maximum value of G'' for the same values of c_v.

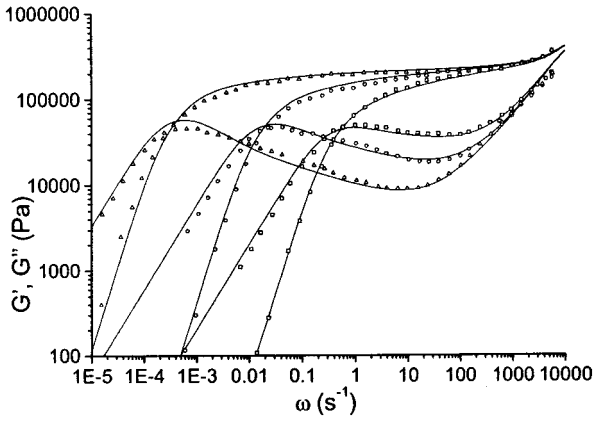

Figure 10. Dynamic moduli for PS from ref 18 and the best fit by the theory.

we predict higher slope for $Z \approx 5..20$ and lower for $Z > 100$. It is not clear whether this contradicts the experimental observations since 3.4 was reported as an average slope over all available molecular weights. We also plotted predictions of Doi $\eta/\eta_{DE} = (1 - 1.47/\sqrt{Z})^3$ to show that it agrees with our theory without CR for $Z > 20$ and the empirical result of Rubinstein−Colby $\eta/\eta_{DE} = 0.11(1 - 1/Z)^{3.8}$, which does not agree with our predictions for $c_v = 1$ even for $Z \to \infty$, which indicates the inconsistency of CLF spectra used in ref 7.

As for the steady-state compliance, we predict nonmonotonic behavior with the maximum at $Z \approx 10$ with the value of J_e about 50−60% higher than J_e at $Z \to \infty$. This is not inconsistent with published data but has not been commented on before, probably because the experimental error in definition of J_e is usually higher than for viscosity and can be about the magnitude of the predicted effect. We would like to stimulate more high-accuracy experiments in the area of mildly entangled chains ($Z = 2-20$) in order to examine the validity of the theory in this region, in particular the approximation used for combining longitudinal modes with other modes in an independent fashion.

We now discuss different experimental quantities usually extracted from G' and G''. The estimate of reptation time or terminal time is defined in three possible ways. First is the inverse frequency of the crossover of G' and G'' which we denote as $\tau_{cross} = 1/\omega_c$: $G'(\omega_c) = G''(\omega_c)$. The second is defined similarly through the position of the maximum of G'', which we denote as τ_{peak}. And the third can be defined as a characteristic of the terminal zone as $\tau_{term} = \lim_{\omega\to 0}(G'(\omega)/(\omega G''(\omega))) \equiv J_e\eta$. A detailed account of the constraint release leads to a wide spectrum of times from τ_e to $\tau_e Z^5$, which makes the experimental procedure of extracting the terminal time from linear spectra a difficult problem. Therefore, we extracted these three times from predicted G' and G'' curves and compared them with the bare reptation time. Figure 9a gives the predictions of each of these three times for different c_v normalized by the bare reptation time $\tau_d^{(0)} = 3Z^3\tau_e$. We note that independent of c_v we predict $\tau_{term} < \tau_{peak} < \tau_{cross}$; however, the difference between them does increase with c_v. We also show that eq 12 describes well all three times without CR (i.e., for $c_v = 0$), and for $c_v = 1$ and $Z \to \infty$ τ_{cross} is decreased about 2 times and τ_{term} about 4 times.

Figure 9b illustrates our discussion of the experimental definition of the plateau modulus $G^{(0)}_{min}$ as a value of G' at the frequency where G'' has a minimum. We plot this value as a function of Z again for three values of c_v. It approaches the value of about $0.78G_e$ for $Z > 150$ and therefore can serve as an approximate measure of G_e. However, we think that the more accurate measure of G_e should be done by fitting of the whole G' and G'' curves by some reliable theory. We also plot the value of G'' at its peak value. It does depend on c_v but however cannot be a good measure of it since presumably the peak shape and height are strongly affected by polydispersity. We leave this to a subsequent paper.

7. Comparison with Experiment

We now compare theoretical predictions for G' and G'' with experimental data available in the literature. In the comparison we use τ_e and G_e as a fitting parameters (same for all samples of fixed monomer chemistry) and calculate M_e from eq 3. We have a choice either to use c_v as an adjustable parameter or to chose it to be the same for all samples and materials. If we set it as a free parameter, we always get values in the range $c_v = 1-2$, but the quality of fitting (weight function) very weakly depends on c_v in this range, and therefore the determination of c_v is not possible from available data. Therefore, we set $c_v = 1$.

Figure 10 shows the best fit of data by Schausbereger et al.[18] for three polystyrenes (PS) of $M_w = 290$K, 750K, and 2540K at $T = 180$ °C. The fitting parameters are $G_e = 2.79 \times 10^5$Pa, $\tau_e = 3.36 \times 10^{-4}$ s, and therefore $M_e = 12.96$K (using $\rho = 959$ kg/m^3 from ref 12.)

Figure 11 shows the best fit of data by Graessley and Roovers[19] for two polystyrenes of $M_w = 275$K and 860K. The fitting parameters are $G_e = 2.69 \times 10^5$ Pa, $\tau_e = 9.22 \times 10^{-4}$ s, and therefore $M_e = 14.47$K. The temperature is $T = 169.5$ °C.

In both cases the agreement is very reasonable. The most pronounced disagreement is observed at the peak of G'' for the highest molecular weight—the worst point is about 25% off in both cases. We also note that the data set by Onogi et al.[20] does not seem to be self-consistent since the ratio of the visual plateau of G' and the maximum value of G'' is very low—about 2.5 instead of 3.5−4 in all other data sets (only G' is plotted in the Doi−Edwards book). We think no theory can explain this because of the implied violation of the Kramers-Krönig relation for G' and G''.

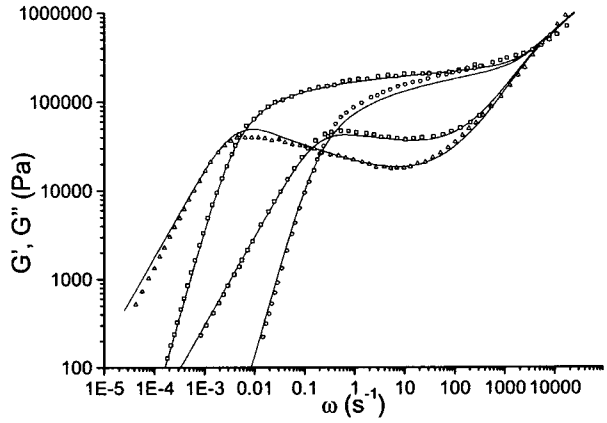

Figure 11. Dynamic moduli for PS from ref 19 and the best fit by the theory.

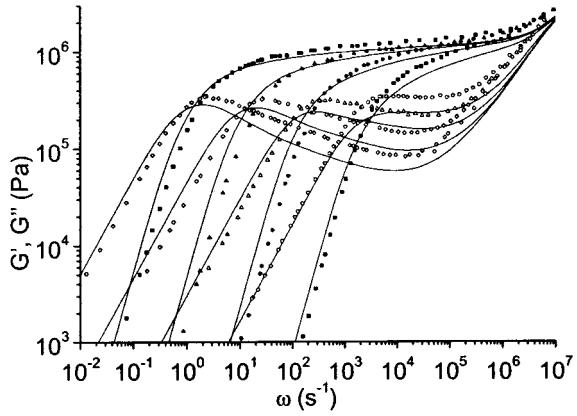

Figure 12. Dynamic moduli for PB from ref 21 and the best fit by the theory constraining the values of G_e and M_e.

Now we consider experimental data available for polybutadiene (PB). Figure 12 shows the data of Baumgaertel et al.[21] for four PB samples of M_w = 20.7K, 44.1K, 97K, and 201K at T = 28 °C. The polydispersity of the first three samples is below 1.07, and for the last one it is 1.27. Since we do not have a polydispersity correction yet, we will fit all samples with our monodisperse theory. We note however that omission of the polydisperse sample does not change the quality of fitting and the conclusions at all. Each sample has about 8% vinyl content.

The fitting parameters are $G_e = 1.43 \times 10^6$ Pa, $\tau_e = 4 \times 10^{-7}$ s, and therefore M_e = 1.57K (using ρ = 896 kg/m^3 from ref 12). It is obvious that the quality of fit is unacceptable: G'' is underestimated in all cases in the intermediate regime, and the terminal zones are not fitted right at all. Changing c_ν does not improve the situation unless c_ν is about 10, which is physically unreasonable and induces a shape in the peak of G'' that looks clearly wrong (see Figure 7).

The situation could be improved if one considers G_e and M_e as an independent parameters. This leads to the much better fit shown in Figure 13, with fitting parameters $G_e = 1.84 \times 10^6$ Pa, $\tau_e = 4.9 \times 10^{-7}$ s, and M_e = 1.93K. This leads to $G_e(M_e) = 1.16 \times 10^6$ Pa; i.e., independent fitting gives an entanglement modulus 60% higher than predicted from M_e by eq 3.

A similar picture is observed with the data for PB samples of Juliani and Archer[22] at T = 26 °C with M_w = 25K, 58K, 95K, 161K, and 395K, plotted in Figure 14. To achieve reasonable agreement, we had to use independent G_e and M_e: $G_e = 2.09 \times 10^6$ Pa, $\tau_e = 2.93 \times 10^{-7}$ s, and M_e = 1.61K. The calculated value of the entanglement modulus is $G_e(M_e) = 1.36 \times 10^6$ Pa. The agreement is not as good as with Baumgaertel's data, and one explanation may be the chemical difference between samples of the series. (We note the scatter at high frequencies and viscosities plotted vs M_w.) However, the main conclusion is the same: independent fitting of G_e and M_e leads to the product G_eM_e higher than expected ρRT by about 50−60%.

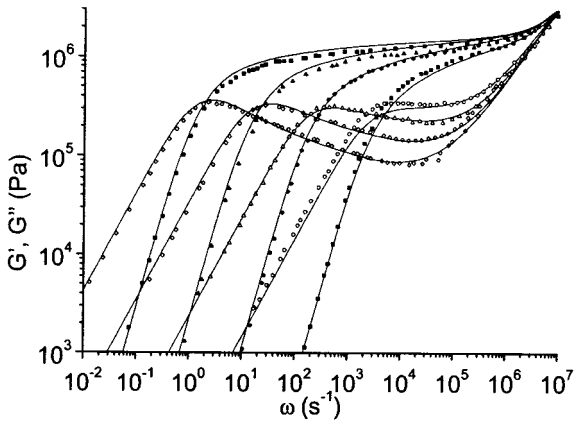

Figure 13. Dynamic moduli for PB from ref 21 and the best fit by the theory using G_e and M_e as an independent fitting parameters.

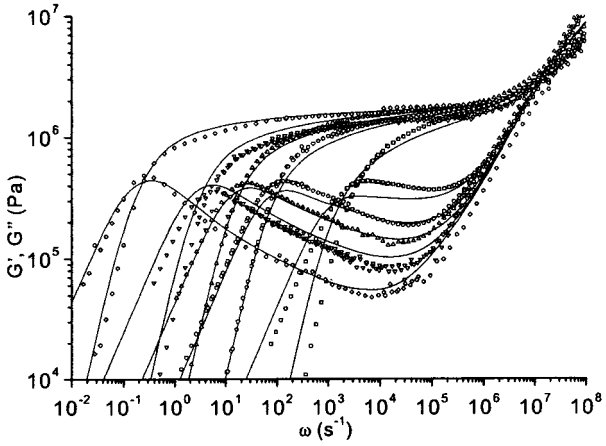

Figure 14. Dynamic moduli for PB from ref 22 and the best fit by the theory using G_e and M_e as an independent fitting parameters.

We conclude that more high-precision data on pure monodisperse samples is needed to confirm our discovered disagreement for polybutadiene but also new data for other monodisperse polymers. The predictions of our theory eq 19 for comparison with experimental data are available from the Web[23] for different c_ν values and for Z = 2−1000.

Finally, in Figure 15 we compare our predictions for viscosity as shown in Figure 8a with the experimental data of Colby et al.[24] for viscosity of polybutadienes of exeptional range of molecular weights. We used parameters listed in discussion of Figure 13 without any fitting. One can see that the agreement is good everywhere except the area of $M_w \approx$ 10 000, which corresponds to about five entanglements. That means that it is possible that for such low values of entanglements effect of discrete nature of entanglements can play a role as well as fluctuations in number of entanglements.

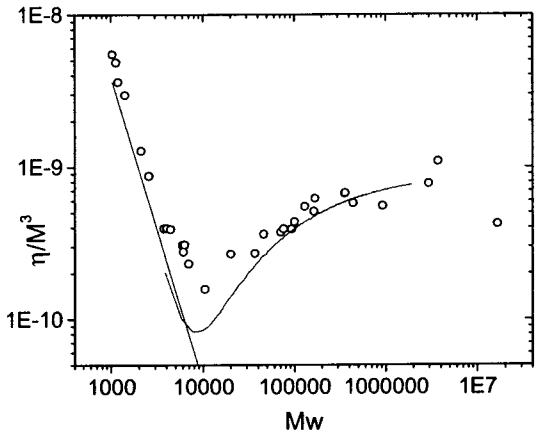

Figure 15. Viscosity of PB measured by Colby et al.[24] and predictions of our theory.

8. Conclusions

In this paper we developed a self-consistent tube theory for linear dynamics of polymer melts which avoids most of the approximations used before. In particular, we have solved the one-chain problem for reptation and contour-length fluctuations which does not have now any adjustable parameters. The contribution to stress relaxation by longitudinal modes is also calculated analytically, and definitions of the entanglement modulus G_e and entanglement molecular weight M_e are proposed which eliminates long-standing confusion with $^4/_5$ prefactors in definitions.

This level of precision allows us to see for the first time the difference between polybutadiene and polystyrene behavior. If for PS the theory describes experimental data rather accurately, for PB one has to chose G_e and M_e which violates eq 3. There can be several explanations of this disagreement. (1) Two polymers have different packing length, yet our theory is universal, i.e., does not take this parameter into account. It might be that the role of contour length fluctuations is different for polymers with different packing length. (2) The randomness in distribution of vinyl groups in PB acts as effective polydispersity of monomer mobilities, which can affect relaxation spectra.

However, our concern is that most of the experimental data do not achieve self-consistency within the 5% accuracy usually claimed. In particular, the procedure of time−temperature superposition is very likely be a cause for a contradiction between different groups. In particular, our own preliminary data for PB samples (to be published) do not exhibit the contradiction observed above. Therefore, we would like to stimulate new high-precision experiments on carefully selected monodisperse samples of different materials, since the existing model (Figure 1) is solved with a high precision, and any consistent disagreement with the reliable well-controlled experiment must mean that a new physical models must be introduced.

Acknowledgment. We thank Alexander Semenov and Ron Larson for fruitful discussions and Lynden Archer for providing us with his data. Funding from the EPSRC μPP program is gratefully acknowledged.

Appendix A. Relaxation of Monomer Density inside the Tube

Let us introduce three variable along the deformed tube: $r(s)$ is the curvilinear distance, s is the segment number, and i is the monomer number. In this notation monomer density inside the tube is

$$\nu(s,t) = \frac{\mathrm{d}i}{\mathrm{d}s} = \left(\frac{\mathrm{d}r}{\mathrm{d}i}\right)^{-1}\left(\frac{\mathrm{d}r}{\mathrm{d}s}\right) \tag{20}$$

The function $r(s)$ does not depend on time (tube is not moving) and is equal to

$$r(s) = \int_0^s |\mathbf{Eu}(s_1)|\,\mathrm{d}s_1 \approx s + \gamma\int_0^s u_x(s_1)\,u_y(s_1)\,\mathrm{d}s_1$$

At $t = +0$ we have $i = N_e s$ and therefore

$$r(i,\, t=+0) = i/N_e + \gamma/N_e\int_0^i u_x(i_1)\,u_y(i_1)\,\mathrm{d}i_1$$

This can be transferred to Rouse coordinates according to standard formulas

$$r(i) = i/N_e + X_0 + 2\sum X_p \cos\left(\frac{\pi p i}{N}\right);$$

$$X_p = \frac{1}{N}\int_0^N (r(i) - i/N_e)\cos\left(\frac{\pi p i}{N}\right)\mathrm{d}i$$

Thus, we obtain

$$X_p(t=+0) = \frac{\gamma}{N}\int_0^N \mathrm{d}i\,\cos\left(\frac{\pi p i}{N}\right)\int_0^{i/N_e} u_x(s_1)\,u_y(s_1)\,\mathrm{d}s_1 = -\frac{\gamma}{\pi p}\int_0^Z u_x(s_1)\,u_y(s_1)\,\sin\left(\frac{\pi p s_1}{Z}\right)\mathrm{d}s_1 \tag{21}$$

where we changed order of integration and calculated the integral over di. But the time dependence of Rouse modes is well-known:

$$X_p(t) = X_p(+0)\,\exp\left(-\frac{p^2 t}{\tau_R}\right)$$

if one neglects fluctuations. Therefore, d$r(i,t)$/di is also known, and we get from eq 20

$$\nu^{-1}(s,t) = \frac{1}{1+\gamma u_x(s)\,u_y(s)}\frac{1}{N_e}\left\{1 + 2\sum_p \frac{\pi p}{Z}\sin\left(\frac{\pi p s}{Z}\right)\exp\left(\frac{-p^2 t}{\tau_R}\right)\frac{\gamma}{\pi p}\int_0^Z u_x(s_1)\,u_y(s_1)\,\sin\left(\frac{\pi p s_1}{Z}\right)\mathrm{d}s_1\right\} \tag{22}$$

This result can be now substituted in eq 17, expanded up to first order in γ, and averaged over all directions of **u**. This procedure leads to a simple formula

$$\sigma(t) = G_e\gamma\left(\frac{4}{5} + \frac{1}{5Z}\sum_{p=1}^{Z-1}\exp\left(-\frac{p^2 t}{\tau_R}\right)\right)$$

which we use in section 5.

Appendix B. A Possible Way To Determine Tube Diameter in Simulations and Incoherent Scattering

One way to define the main parameter of the tube theory, the tube diameter a, is through the monomer mean-square displacement $\phi(t)$ for $t < \tau_e$ and $t > \tau_e$.

At times smaller than the Rouse time of one entanglement segment $t < \tau_e$ our model assumes free Rouse

motion, and therefore

$$\phi(t) = \frac{1}{N}\int_0^N \langle (R_m(t) - R_m(0))^2 \rangle \, \mathrm{d}m = \frac{2Nb^2}{\pi^{3/2}}\sqrt{\frac{t}{\tau_R}} = \frac{2b^2}{\pi^{3/2}}\sqrt{\frac{t}{\tau_0}} \sim t^{1/2}$$

where $\tau_0 = \tau_R/N^2$ (see, for example, ref 2, eq 4.III.6).

At later time $\tau_e < t < \tau_R$ the monomer travels in a tube of persistence length a, and in time t it will pass through a contour length $\sqrt{\phi(t)/3}$ or $n(t) = \sqrt{\phi(t)/3}/a$ tube segments. The factor of 3 appears because in a tube the motion takes place only in one dimension and the other two are suppressed. Therefore, the monomer mean-square displacement will be

$$\phi^{\mathrm{tube}}(t) = n(t)a^2 = a\sqrt{\frac{\phi(t)}{3}} \sim t^{1/4}$$

Now if one fits the short time behavior with a function proportional to $t^{1/2}$ and the long time with $t^{1/4}$ (straight lines in log−log plot), then the intersection of these two lines will be at ϕ^* and t^*, which are determined as

$$\phi^{\mathrm{tube}}(t) = \phi(t) \rightarrow a\sqrt{\frac{\phi(t)}{3}} = \phi(t) \rightarrow \phi^* = \frac{a^2}{3} \quad (23)$$

Therefore, this intersection gives neither exactly the tube radius nor the tube diameter. The time of the intersection is also not τ_e but

$$t^* = \frac{\pi^3}{36}\tau_e \quad (24)$$

We think that this well-known argument is the best way to find the tube diameter a from microscopic consideration. This is easy to realize in computer simulations[25] and also possible to obtain from incoherent neutron scattering. We note that a defined using eq 23 is in fact a persistence length of the tube (or primitive path) and therefore does not require assumptions about the mean field profile which creates a tube in a direction perpendicular to the primitive path. The relations $N_e b^2 = a^2$ and $G_e = \rho RT/M_e$ are less robust since the first can be violated if N_e is not big enough to consider the entanglement segment as a Rouse chain and the second if deformation is not affine or entanglement points fluctuate in space. Also, one may argue that the tube diameter may not be equal to the tube persistence length from eq 23. However, the diameter of the tube is not a well-defined quantity since the tube is a fuzzy object with density smoothly decaying to zero. This is also why we do not see any strong arguments why our constraint release parameter c_ν should be exactly equal to one.

References and Notes

(1) de Gennes, P. G. *J. Chem. Phys.* **1971**, *55*, 572.
(2) Doi, M.; Edwards, S. F. *The Theory of Polymer Dynamics*; Clarendon: Oxford, 1986.
(3) de Gennes, P. G. *J. Phys. (Paris)* **1975**, *36*, 1199.
(4) Doi, M. *J. Polym. Sci., Polym. Lett. Ed.* **1981**, *19*, 265.
(5) Doi, M. *J. Polym. Sci., Polym. Phys. Ed.* **1983**, *21*, 667.
(6) Milner, S. T.; McLeish, T. C. B. *Phys. Rev. Lett.* **1998**, *81*, 725.
(7) Rubinstein, M.; Colby, R. H. *J. Chem. Phys.* **1988**, *89*, 5291.
(8) Everaers, R. *Eur. Phys. J. B* **1998**, *4*, 341.
(9) Ketzmerick, R.; Ottinger, H. C. *Coninuum Mech. Thermodyn.* **1989**, *1*, 113.
(10) O'Connor, N. P. T.; Ball, R. C. *Macromolecules* **1992**, *25*, 5677.
(11) Graessley, W. W. *Polym. Sci., Polym. Phys. Ed.* **1980**, *18*, 27.
(12) Fetters, L. J.; Lohse, D. J.; Milner, S. T.; Graessley, W. W. *Macromolecules* **1999**, *32*, 6847.
(13) des Cloizeaux, J. *Macromolecules* **1990**, *23*, 46787.
(14) Likhtman, A. E.; Milner, S. T.; McLeish, T. C. B. *Phys. Rev. Lett.* **2000**, *85*, 4550.
(15) Dean, P. *Proc. Phys. Soc.* **1964**, *84*, 727.
(16) Pattamaprom, C.; Larson, R. G.; Van Dyke, T. J. *Rheol. Acta* **2000**, *39*, 517.
(17) Brochard-Wyart, F.; Ajdari, A.; Leibler, L.; Rubinstein, M.; Viovy, J. L. *Macromolecules* **1994**, *27*, 803.
(18) Schausberger, A.; Schindlauer, G.; Janeschitz-Kriegl, H. *Rheol. Acta* **1985**, *24*, 220.
(19) Graessley, W. W.; Roovers, J. *Macromolecules* **1979**, *12*, 959.
(20) Onogi, S.; Masuda, T.; Kitagawa, K. *Macromolecules* **1970**, *3*, 109.
(21) Baumgaertel, M.; De Rosa, M. E.; Machado, J.; Masse, M.; Winter, H. H. *Rheol. Acta* **1992**, *31*, 75.
(22) Juliani, Archer L. A. *J. Rheol.* **2001**, *45*, 691.
(23) See Web page: irc.leeds.ac.uk/~phyall/linlin.htm. We also will be happy to fit your new or old data if you send it to A.Likhtman@leeds.ac.uk.
(24) Colby, R. H.; Fetters, L. J.; Graessley, W. W. *Macromolecules* **1987**, *20*, 2226.
(25) Putz, M.; Kremer, K.; Grest, G. S. *Europhys. Lett.* ***2000***, *49*, 735.

MA0200219